Kobe University Repository : Kernel

PDF issue: 2026-11-20

Experimental Study on Prestressing Force of Corroded Prestressed Concrete Steel Strands

Li, Jingyuan
Miki, Tomohiro
Yang, Qiuning
Mao, Mingjie

(Citation)
Journal of Advanced Concrete Technology,20(9):550-563

(Issue Date)
2022-09-06

(Resource Type)
journal article

(Version)
Version of Record

(Rights)
© 2022 by Japan Concrete Institute

(URL)
https://hdl.handle.net/20.500.14094/0100492457

KOBE UNIVERSITY

Scientific paper

Experimental Study on Prestressing Force of Corroded Prestressed Concrete Steel Strands

Jingyuan Li[1], Tomohiro Miki[2*], Qiuning Yang[3] and Mingjie Mao[3]

Received 2 May 2022, accepted 16 August 2022 doi:10.3151/jact.20.550

Abstract

This study presents the effect of corrosion of prestressed concrete (PC) strands on the prestressing force and the reduction mechanism of the uniaxial force. A total of 14 strands was tested by combining a rigid frame testing machine with an electrified accelerated corrosion device. The specimens were divided into two groups having prestressing levels of 70% and 50% of tensile strength of PC strands. The expected degree of corrosion of the specimens, which was defined by the mass loss, was calculated from controlled electric current and time. A rigid frame testing machine was used to sustain the tensile force of the PC strands, and the prestressing force and deformation of the strand were continuously measured during the corrosion test. The test results indicate that the prestressing force decreases with the increase of corrosion. After the corrosion tests, tensile loading tests were carried out on the specimens that did not rupture during the corrosion test. It was found that corrosion led to the deterioration of the tensile properties of the PC strands, and the ultimate tensile capacity of the corroded PC strand was related to the fracture condition.

1. Introduction

Prestressed concrete (PC) steel strands have high tensile strength and are widely used in important structural members of PC bridges (Lee *et al*. 2020). For instance, the cables of suspension bridges are made from multiple strands, and the structural capacity and serviceability of PC bridges can be improved using prestressing tendons. There have been a series of failures of PC bridges all over the world, such as the Nielsen Strait Bridge in the United States, the Saint Stefano Bridge in Italy, and the pedestrian bridge at Lowe's Motor Speedway in North Carolina (Darmawan *et al*. 2007; Proverbio *et al*. 2000; Cederquist 2000). Most of these accidents were caused by the corrosion of PC steel strands. Corrosion has become one of the biggest threats to structural safety (Biondini and Frangopol 2018). Therefore, it is of great significance to study the mechanical properties of corroded PC steel strands and the law of prestress degradation to grasp and predict the performance degradation and failure characteristics of PC structures.

Kondo *et al*. (2016) have simulated the reduction in the cross-sectional area of PC steel strands due to corrosion by artificially cutting the steel strands. Tensile tests were carried out on the cut and corroded strands separately to compare the differences in performance between them. The test results showed that as compared with the corroded PC steel strand, the maximum load of the cut steel strand had a linear relationship with the elongation when the cross section of the cut steel strand was reduced less.

The mechanical properties of corroded PC strands have been reported by Kitano *et al*. (2007). According to the degree of corrosion in this test, the steel strand was divided into four categories: less than 1%, 1% to 2.5%, less than 10%, and more than 10%. The influence of the degree of corrosion on the tensile strength, yield strength, elastic coefficient, and elongation of the steel strand was observed. The report indicated that even if the mass loss rate is the same, the mechanical properties of the steel strand with different corrosion characteristics are different. The steel strand with slight surface corrosion was similar to the steel strand without corrosion, but the performance of the steel strand with pitted corrosion deteriorated obviously. The tensile and yield strengths of corroded PC steel strand decreased with the increase of mass loss, and similar conclusions can be obtained by showing the section loss.

Kuga *et al*. (2012) used the electrified accelerated corrosion method to corrode steel strands embedded in concrete, set seven corrosion levels at 0% and from 10% to 40%, and carried out tensile tests to analyze the effect of corrosion on the maximum tensile strength, yield strength, stiffness and elongation rate of steel strand. They have found that the maximum tensile strength and yield strength decreased with the increase of the degree of corrosion.

In aggressive environments, PC steel strands were more prone to corrosion under high stress conditions (Wang *et al*. 2014). However, most of the earlier studies ignored the promotion of prestress on the corrosion of steel strands in the actual working condition, especially under prestressing situations. Jeon *et al*. (2019) con-

[1]Graduate Student, Department of Civil Engineering, Kobe University, Kobe, Japan.
[2]Associate Professor, Department of Civil Engineering, Kobe University, Kobe, Japan. *Corresponding author, *E-mail*: mikitomo@port.kobe-u.ac.jp
[3]Professor, School of Civil and Hydraulic Engineering, Ningxia University, Yinchuan Ningxia, China.

Table 1 Material properties of steel strand.

Type	Nominal diameter	Cross-section area	Weight per meter	Tensile strength	Range of ultimate tensile capacity*	Elongation
1×7	15.2 mm	140 mm^2	1101 g/m	1860 MPa	260 to 288 kN	≥3.5%

*Note: The range of the ultimate tensile capacity is shown based on the standard. As a reference, the ultimate tensile capacity of the one PC strand was 265 kN based on the tensile loading test.

ducted tensile tests on prestressing steel strands in external tendons of the existing bridge in service. The amount of decrease in tensile strength was larger than the amount of decrease in the reduction in cross sectional area, and the decrease of fracture strain was large enough to be cautious. Zhang *et al*. (2017a) used the artificial climate corrosion method to corrode steel strands with prestressing applied to investigate their mechanical properties and found that corrosion resulted in a significant reduction in the ultimate strain of the strands, leading to brittle damage. In contrast, the effect of corrosion on the elastic modulus and yield strength was not obvious in the previous study. For instance, Wang *et al*. (2020) also used the artificial climate corrosion method to corrode the PC steel strands, analyzed the shape of corrosion and its mechanical properties, and found that high stress levels can promote the expansion of corroded microcracks on the surface of steel strands. Finally, the corrosion was divided into slight and severe conditions, and a constitutive model was proposed to predict the stress-strain curve of these corroded PC strands.

Prestressing force of the PC steel strands is an important component of prestressed members and has a great influence on the mechanical properties of PC structures. However, there are few research works on how corrosion affects prestress and the law of its effect. Zhang *et al*. (2017b) have investigated the flexural behavior of bonded post-tensioned concrete beams under strand corrosion, and they have found the reduction of flexural properties of beams after corrosion and inferred the loss of prestress by calculation. The effect of corrosion on prestress in PC strand needs to be further studied.

The objective of the present study is to investigate the effect of corrosion on prestressing force in PC strands and the mechanism of the stress redistribution in the strand. This paper innovatively combines an electrochemically accelerated corrosion device with a relaxation test machine, which can directly observe the change of prestress during the corrosion process. According to the prestress, total 16 steel strands were divided into two groups, and the prestressing force and deformation of strands were continuously measured to study the level of prestress change. This study presents an investigation on the prestress loss mechanism of steel strands caused by corrosion and provides a reference for durability for corroded PC structures.

2. Experimental program

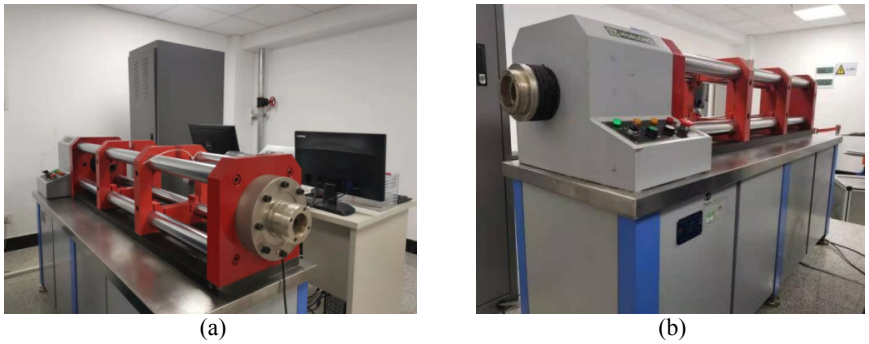
2.1 Details of specimens

In this section, first the material properties are introduced, then the special electrochemically accelerated corrosion test is explained. Herein, combining a relaxation test machine and a traditional electrochemically accelerated corrosion test, the PC strands in the working status were investigated regarding the prestressing force, and the elastic modulus was measured. After conducting the corrosion test, the tensile test was conducted for some corroded prestressed steel strands that were not ruptured during the corrosion tests.

Specimens were fourteen 15.2 mm diameter 7-wire steel strands. The length of the strand samples was set as 2.5 m to adapt to the relaxation loading test machine. The material performances of the strand are given in **Table 1**.

2.2. Accelerated corrosion test

In order to measure the change of prestressing force and elastic modulus of PC steel strand in the corrosion process under working conditions, the relaxation testing machine WSC-300 and electrochemically accelerated corrosion device were combined in the test. Tension steel strands to simulate the high prestressed working condition of strands in PC beam, and the prestressing force in the strand was continuously measured. The relaxation test machine used here is shown in **Fig. 1**. The anchorages of the machine used were fixed with the



(a) (b)

Fig. 1 Microcomputer controlled tensile stress relaxation testing machine WSC-300.

steel strands on both ends. The side shown in **Fig. 1(b)** can move to stretch strands, and it stops moving when prestressing force reaches target values. The displacement of two anchorages was kept constant during the test process.

In general, the accelerated corrosion methods can be divided into three conditions: electrochemical accelerated corrosion, dry-wet alternating corrosion, and artificial climate box corrosion. The strands were corroded uniformly by means of the electronic accelerate method than steel strands in natural environments. In most situations, the effect of reduction of the cross-sectional area caused by two corrosion methods on strand properties may be regarded as similar.

Due to the existence and limitation of the relaxation machine, the latter two methods are difficult to use, and the electrochemically accelerated corrosion method has the advantages of simple operation, short corrosion cycle, low cost, accurate control of the degree of corrosion, and the most important thing is that it can be more convenient to combine with relaxation testing machine test.

Fourteen corroded steel strand specimens were used to study the influence of corrosion on the prestress and mechanical properties of steel strands. Faraday's electrolysis law was used to calculate the corrosion time, and specimens with different degrees of corrosion were obtained by controlling the corrosion time and current intensity. Faraday's first law of electrolysis can be expressed as,

$$\Delta w = \frac{M}{NF} IT \tag{1}$$

where Δw is the mass of metal corrosion; I is the current intensity; M is the atomic mass of metal; F is the Faraday constant (F = 96485); N is the number of valence electrons lost by oxidation of a metal; T is the corrosion time.

Faraday's law is used to calculate the theoretical mass of metal corrosion. Eq. (1) can be translated into Eq. (2) to calculate mass loss as the degree of corrosion.

$$n = \frac{M}{NFm_0} IT \tag{2}$$

where n is the calculated mass loss of the corroded steel stands and m_0 is the initial mass of the corroded steel strands. Equation (2) can be written as $T = \frac{nNFm_0}{MI}$ to calculate the corrosion time.

Table 2 Grouping of specimens.

Series	Symbol	Target degree of corrosion %	Corrosion time h	Stress level
70-series	70-0-1	0	0	$0.7\sigma_s$
	70-2-1	2	30	
	70-2-2	2	30	
	70-5-1	5	75	
	70-5-2	5	75	
	70-5-3	5	75	
	70-10-1	10	150	
	70-10-2	10	150	
	70-10-3	10	150	
50-series	50-0-1	0	0	$0.5\sigma_s$
	50-5-1	5	75	
	50-5-2	5	75	
	50-5-3	5	75	
	50-10-1	10	150	
	50-10-2	10	150	
	50-10-3	10	150	

Note: σ_s is the tensile strength of the steel strand.

The detailed group of the specimens is shown in **Table 2**. To study the influence of different degrees of corrosion on the steel strand of different prestress grades, the specimens are divided into two series: 70-series and 50-series.

The initial tension stress of the strand was used to reflect the prestress level in the present study. The initial tension stress of series 70 and 50 were 70% and 50% of σ_s, respectively, where σ_s is the tensile strength of the steel strand. The 70-series contained 3 groups, and the 50-series contained 2 groups. Each group consisted of three strand samples except for 70-2, which includes 2 samples.

The test device is shown in **Fig. 2**, and the diagram of the test setup is shown in **Fig. 3**. The 100×100×500 mm mold is installed in the center of the relaxation test machine as a tank filled with water to corrode the steel strands at 500 mm in the middle. The corrosion system consisted of the direct current galvanostatic, the strand anode, and the stainless-steel cathode submerged in the 5% saline solution.

Drill holes on both sides of the tank so that the strand passes through it, apply structural adhesive to the edges

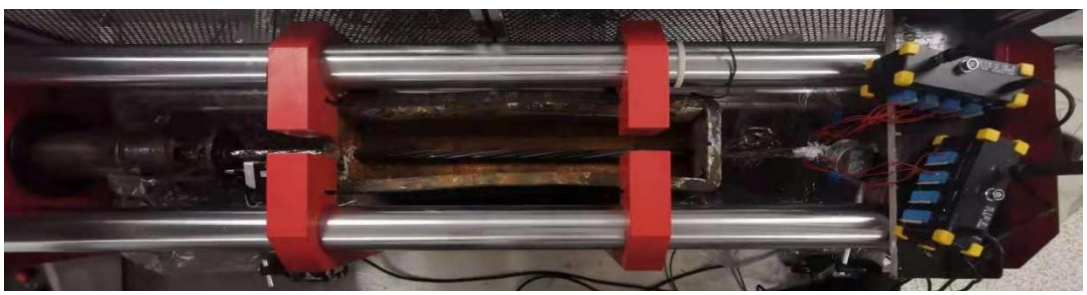


Fig. 2 Corrosion test setup with a relaxation test machine.

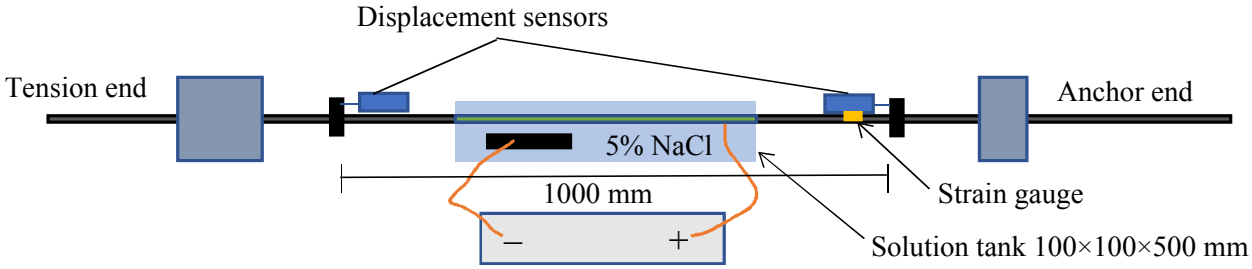


Fig. 3 Outline of corrosion test under sustain tensile loading.

of the holes between the strand and the mold to prevent sodium chloride solution from leaking out, and wrap the non-corroded part of the strand with transparent tape to prevent the solution from flowing out along the internal pores of the strand. The fixed steel plate was installed on the steel strand has a displacement along with the elongation of the steel strand. The displacement of the steel plate in the test process is measured by the sensor, that is, the longitudinal deformation of the steel strand. The initial distance of the sensor was set as 1 m, and the initial tension distance of the relaxation machine was set as 1.5 m. Epoxy resin is applied to the anchor end of the relaxer to prevent the anchor end from corrosion. To ensure that the current will not affect the normal operation of the relaxer, the corrosion current was smaller at 0.5 A or 0.35 A. When the tensile force reached target values, most specimens started the corrosion test. The 70-10-2, 70-10-3, and 50-10-1 started the corrosion test after 10 hours when the tensile force was applied. During the corrosion test, the distance between the two anchorage ends remained constant. The corrosion tests were terminated when wires were fractured or specimens reached the target degree of corrosion.



Fig. 4 Microcomputer controlled electro-hydraulic servo universal testing machine (Model SHT4106G).

2.3 Tensile loading test

A tensile loading test was carried out on 9 steel strands that showed without fracture during the previous corrosion test. The electric hydraulic servo universal testing machine as shown in **Fig. 4** was used to tension the steel strand. To facilitate the tensile test, the test strands were cut to 1000 mm (including the corroded section) and protected at both ends with clamps. In the tensile test, two end sides of the strand are held by the grip. If the grip wedge contacts the surface of a strand directly, a crack can be propagated from the wedge earlier than the tensile strength of the wire due to stress concentration. For this reason, Kim *et al*. (2014) suggested wrapping the end parts with a silica-coated aluminum sheet to protect the end parts. This method was adopted in this study. The loading speed was controlled by displacement and was set at a rate of 1 mm/min. The load data was automatically read by the tension tester.

Strand was considered to reach the ultimate tensile force once the steel wire was ruptured as stipulated in the Chinese Standard GB/T 5224-2014. The failure modes of specimens with different degrees of corrosion were compared to investigate the fracture mode of steel wire under different corrosion losses. The relationship between the ultimate tensile strength and the degree of corrosion curve was drawn to summarize the effect of corrosion on the tensile capacity of the strand. For the steel strand failed in the tension test, the corroded section was re-intercepted after the test, cleaned with 12% hydrochloric acid, and measured the weight to calculate the mass loss of the corroded steel wires. The tested wires in the PC strand are shown in **Fig. 5** as a sample.



Fig. 5 Disassembled corroded steel wires.

Table 3 Corrosion test result.

Specimen No.	Prestress degree	Mass loss %	Mass loss of fractured wire %	Prestress loss %	Test series the wire was ruptured (see Notes below)
70-0-1	70% (182 kN)	0.0	0.0	0.76*	-
70-2-1		2.0	2.7	2.2	T
70-2-2		1.9	3.7	2.4	T
70-5-1		6.0	6.2	2.8	T
70-5-2		4.5	5.0	3.5	T
70-5-3		4.5	5.3	3.2	T
70-10-1		9.0	10.5	7.4	C
70-10-2		8.2	9.5	5.7	C
70-10-3		5.8	9.6	3.3	C
50-0-1	50% (130 kN)	0.0	0.0	0.66*	-
50-5-1		5.6	5.9	3.2	T
50-5-2		5.1	6.2	3.5	T
50-5-3		7.2	7.5	3.6	T
50-10-1		8.5	9.9	4.5	C
50-10-2		7.8	8.8	3.7	T
50-10-3		8.4	9.1	4.0	T

Notes:
Test series the wire was ruptured: C means failure in the corrosion test and T means failure in the tensile loading test.
*Prestress loss caused by relaxation (the prestress loss of 70-0-1 and 50-0-1 were calculated by the data at 96 hours).

3. Results and discussion of corrosion tests

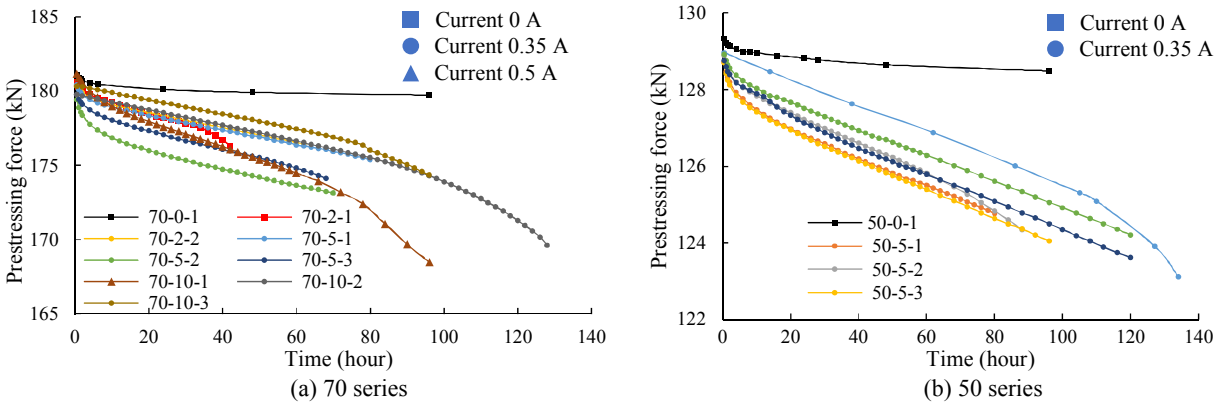
3.1 Results of corrosion tests

Fourteen steel strands were subjected to electrochemically accelerated corrosion under the action of corresponding tensile stress, and the test results are shown in **Table 3**. Due to the effect of bond stress and concrete cracks, there are some differences in prestress loss caused by corrosion between the PC strands and concrete in the PC structures. The mass loss and maximum cross-sectional loss of strands or wires are generally two main parameters to reflect the corrosion level. The mass loss in this study presents the average corrosion level of the PC strand, which is more suitable for the uniform corrosion or global corrosion of samples. In contrast, the maximum cross-sectional loss can reflect the severity of local corrosion and is suitable for reflecting pitting corrosion of samples. In the experiments, the fracture of steel wires was a sign of the failure of PC steel strands, so the mass loss of fractured steel wire can better reflect the damage of the steel strand than the mass loss of the whole strand.

Consider the three specimens 70-10-1, 70-10-2, and 70-10-3 that were corroded to fracture as an example. The mass loss was quite different, but the difference in fracture wires' mass loss was quite small. However, the prestressing force was influenced by the properties of the whole steel strand, and the mass loss of the whole strand has a better correlation with the loss of prestress. Therefore, the mass loss of whole strands was focused on to express the degree of corrosion in this study.

3.2 Prestressing force versus corrosion time

The prestressing force of the specimen with two prestress levels was measured during the corrosion test and is summarized in **Fig. 6**. For uncorroded specimens 70-0-1 and 50-0-1, the prestressing force slightly decreased at early hours due to the relaxation and then almost never decreased continuously. As for corroded specimens, the prestressing force of both groups declined continuously as the corrosion time went by.



(a) 70 series (b) 50 series

Fig. 6 Prestressing force versus corrosion time curve.

Table 4 Measured and calculated mass losses (degrees of corrosion).

Specimen No.	70-2-1	70-2-2	70-5-1	70-5-2	70-5-3	70-10-1	70-10-2	70-10-3
Measured mass loss (%)	2.0	1.9	6.0	4.5	4.5	9.0	8.2	5.8
Calculated mass loss (%)	2.8	4.1	5.3	4.7	4.5	9.1	8.5	6.4
a	0.71	0.46	1.13	0.98	0.99	0.99	0.96	0.91

Specimen No.	50-5-1	50-5-2	50-5-3	50-10-1	50-10-2	50-10-3
Measured mass loss (%)	5.6	5.1	7.2	8.5	7.8	8.4
Calculated mass loss (%)	5.3	5.9	6.4	8.9	8.0	8.0
a	1.05	0.87	1.12	0.96	0.98	1.05

Among them, specimen 70-10-1 used a corrosion current of 0.5 A, which made the corrosion faster, leading to the prestressing force dropping faster than the other specimens. The prestressing force of most of the specimens decreased rapidly in the initial stage of the corrosion test, which was due to an effect of the relaxation of the steel strand. While specimens 70-10-3, 70-10-2, and 50-10-1 were corroded after 10 hours under tension, the effect of relaxation properties on prestressing force almost disappeared and did not show a stage of the rapid decline of prestressing force at the initial stage but declined steadily in a linear relationship with the growth of corrosion time. For the specimens 70-10-1, 70-10-2, 70-10-3, and 50-10-1, which were finally fractured during the corrosion test, as the increase of corrosion time, the prestressing force decreased rapidly. In addition, the maximum cross-sectional area loss was serious, and the strand tensile properties were reduced when the plastic deformation occurred at the section of corrosion pitting, resulting in an accelerated decline in prestress. Specimens 70-10-1 and 70-10-2 had large deformation at the corrosion pitting, and the prestressing force dropped severely during the destruction stage, while specimens 70-10-3 and 50-10-1 had a small deformation at the corrosion pitting and the prestressing force reduced relatively small.

3.3 Calculated degree of corrosion

One of the significant advantages of the widely used accelerated corrosion method is that the theoretical mass of corroded steel strand can be calculated according to Faraday's first law of electrolysis based on the current intensity and corrosion time.

According to Eq. (2), the time history of the degree of corrosion was calculated by corrosion time and current intensity, and the relationship between prestressing force and time was transformed into the relationship between prestressing force and degree of corrosion.

Comparisons between the measured and calculated mass losses due to corrosion are summarized in **Table 4**. It is found that the calculated values of most specimens are close to the measured values. According to Eq. (2), it can be found that the degree of corrosion is linearly related to the corrosion time. The previous section mentioned that the prestressing force linearly declines with the increase in corrosion time, so it can be considered that the prestressing force linearly declines with the increase in the degree of corrosion. The accuracy of Faraday's law is affected by a variety of factors, such as chloride ion concentration, current density, temperature, etc. In this test, the calculated values of some specimens differ greatly from the actual values due to the crystallization cleaning of the corrosion tank and the change of weather and temperature.

However, it can be seen from **Fig. 6** that the relationship between prestressing force and corrosion time is also linear for specimens with different calculated values and measured values, so it can be assumed that the relationship between corrosion time and degree of corrosion is also linear, but the slope is different. Thus, Eq. (2) can be written as;

$$n = a\frac{M}{NFm_0}IT \tag{3}$$

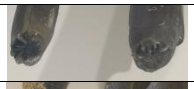
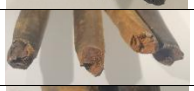
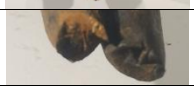
where a is a variable parameter for each specimen and obtained as the measured mass loss divided by the calculated mass loss based on Eq. (2).

3.4 Failure mode of corroded strands in the corrosion tests

The failure modes of the ruptured steel strand during the corrosion test are analyzed. The failure conditions of the four corroded strands are summarized in **Fig. 7**. It can be found from the figure that different from the uniform corrosion of steel bars in the state without prestressing (Feng *et al*. 2021; Hong *et al*. 2020). The corrosion on the surface of the steel strand was not uniform despite adopting the electrochemically accelerated corrosion method. The corrosion of steel wire around the fracture was severe, and the corrosion pitting occurred wide and deep, while the degree of corrosion of other parts of the steel strand was slight, the fracture position of the steel strand was random, and the steel wire became slender at the fracture point, and the fracture is either neat or staggered. It is because the steel strand produced micro-cracks after corrosion, and its local tensile performance decreased, and the high prestress level damage to the weak position further strengthened the corrosion effect. The steel strand deformation occurred in the place where the cross-sectional area loss was greater, and the corrosion condition at the fracture position was more serious than at other positions.

All the fracture types can be divided into three basic

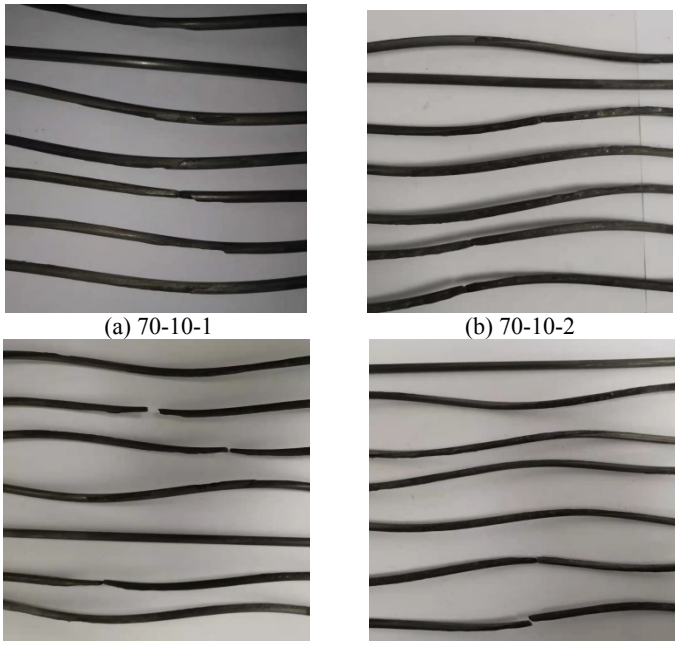
Table 5 Fracture condition of corroded steel wires after corrosion test.

Specimen No.	Fracture section	Fracture types	Necking degree	Mass loss %	Prestress loss %
70-10-1		Milling cutter type	Severe	9.0	7.4
70-10-2		Milling cutter type Cup and cone type	Severe	8.2	5.7
70-10-3		Split type	None	5.8	3.3
50-10-1		Milling cutter type Split type	Slight	8.5	4.5

fracture types: cup and cone type, milling cutter type, split type, and their combination. Macroscopic photos of various fracture types are shown in **Fig. 8**. Cup and cone fracture type consists of cup and cone conjugate. A cup consists of a bottom and a wall (also known as a clipped lip). Some have a wide, flat bottom, while others have a narrow, v-shaped bottom. The milling cutter fracture type consists of many "small ridges" radially distributed along the transverse radius line. Split fracture is composed of several split surfaces, the color is relatively bright.

Necking phenomenon appears near both cup and cone fracture type and milling cutter fracture type (the necking degree of the cup and cone type is relatively light). Both are a ductile failure. There is no obvious necking phenomenon near split type and split-milling cutter type, which belong to brittle failure.

The cross-sectional conditions of the four specimens are shown in **Table 5**. it can be found that 70-10-1 is milling cutter fracture, and 70-10-2 is milling cutter fracture and milling cutter-cup and cone fracture. Both of them showed necking phenomenon near the fracture, and they were ductile fracture; for 70-10-3 and 50-10-1, they were splitting fracture and split-milling cutter type, respectively, they are not obvious necking phenomenon near the fracture, belong to the brittle fracture. There-



(a) 70-10-1 (b) 70-10-2

(c) 70-10-3 (d) 50-10-1

Fig. 7 Corrosion condition of the steel wires.



Cup and cone type | Milling cutter type | Split type | Split-milling cutter type

Fig. 8 Fracture types of corroded steel wires.

fore, the steel wire in the corrosion strand could occur both ductile fracture and brittle fracture.

3.5 Effect of corrosion on prestressing force

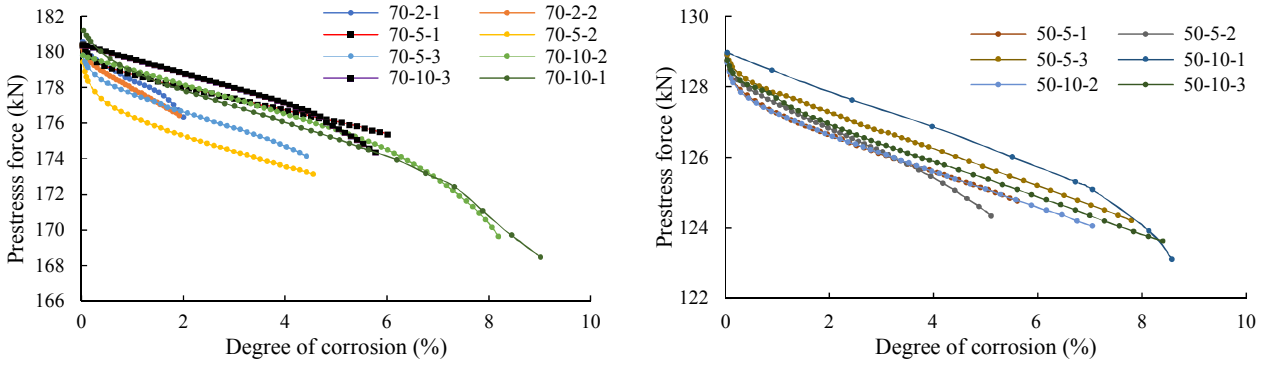
The relationship between the degree of corrosion calculated by Eq. (3) and prestressing force is shown in **Fig. 9**, in which the parameter of a for each specimen was calculated separately. It can be found from the figure that the prestressing force decreases continuously with the increase of the degree of corrosion, but this graph does not remove the effect of relaxation property on prestress, so it can be found that the prestressing force of the strand except for specimens 70-10-3, 70-10-2 and 50-10-1 decreased rapidly at the initial stage, and after 5 to 6 hours. After the degree of corrosion reached around 0.8%, the effect of relaxation property on prestressing force almost disappeared, and prestressing force decreased linearly with the increase of degree of corrosion. As the corrosion of the strand increased, the cross-sectional area decreased, and a large amount of plastic deformation occurred. When the corrosion became severe, the prestressing force decreased rapidly until the specimen failed.

To compare the prestress deterioration of specimens with different prestress degrees, a prestress ratio, P_c/P_0 that is a ratio of prestressing force of corroded strands to that of the uncorroded strands, is defined in the present study and is shown in **Fig. 10**. Comparing the prestress ratios of 70-series and 50-series, the deterioration pattern of prestressing force is the same for both prestress levels of the strands, while the loss of prestressing force in the strand at the 70-series prestress level is more severe than in the 50-series with the same degree of corrosion. The difference increased as the degree of corrosion continued to rise, and the maximum difference was 64.3%.

Figure 11 summarizes the prestress loss versus degree of corrosion when the corrosion test was terminated. A similar pattern can be observed so that the prestress loss became larger as the degree of corrosion increased, although the prestress loss was slightly larger in 70-series than in 50-series at the corrosion level of around 8% or more. This is because when the strand was severely corroded, the corrosion pits produced a large amount of plastic deformation and the prestressing force decreased rapidly.

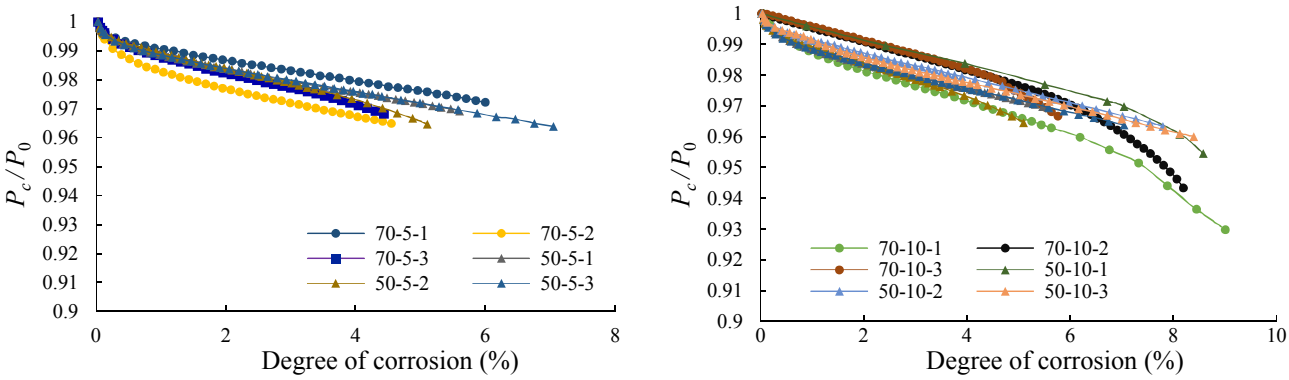
3.6 Reduction process for prestressing force of corroded PC strand

The whole process of prestressing force with increasing degree of corrosion can be divided into three stages, as shown in **Fig. 12** for specimen 70-10-1 as an example. In the first stage, the prestressing force decreases rapidly due to the influence of relaxation properties and corrosion. In the second stage, the strand relaxation properties have almost no effect on the prestressing



(a) 70-series (b) 50-series

Fig. 9 Prestressing force versus degree of corrosion.



(a) 5% corrosion (b) 10% corrosion

Fig. 10 Prestress ratio versus degree of corrosion.

force, and the prestressing force decreases linearly under the action of corrosion. As for the third stage, with the increase in the degree of corrosion, the maximum cross-sectional area of the strand is severely reduced. In this stage, the tensile properties are reduced. When the yield strength is reduced to less than the prestress, the strand shows plastic deformation, and then the prestressing force is significantly reduced. The specimens that are not corroded severely do not reach this stage. This phenomenon may occur in the electronic accelerate corrosion method. The strand was corroded more uniformly reproduced by the electronic accelerate method as compared with that under natural environments. Thus, if the strands that were corroded by two methods have the same mass loss, the cross-section loss of those that were corroded in natural environments is more severe than that were corroded by the electronic accelerate method. The prestress deteriorated process of steel strands under natural environments needs further study.

The first stage, therefore, ends when the effect of strand relaxation performance on the prestress disappears, independent of the degree of corrosion, 70-10-2, 70-10-3, and 50-10-1 three specimens do not have this stage because corrosion began 10 hours after tensioning, while the second stage is completely caused by corrosion to reduce the prestressing force of the strand, and the relationship between them is linear. The reason for the emergence of the third stage is that severe corrosion causes plastic deformation of steel strands, which makes prestressing force decrease rapidly. It was observed that the fracture occurred in the most corroded and deformed wires. Therefore, as compared with the mass loss of the whole strand, the expression of the degree of corrosion by the mass loss of fractured steel wire can more accurately reflect the degradation law of prestress in the third stage.

The corrosion law of fractured wires can be assumed to correspond to the Faraday's first law of electrolysis in this study. The degree of mass loss of fractured wires at each time was calculated by Eq. (3) to show the process of mass loss during the corrosion test, as shown in **Fig. 13**. It can be seen from this figure that the beginning of the third stage of prestressing force was more regular when the degree of corrosion was expressed by the mass loss of fractured wires. The mass loss of the fractured wires at the beginning of the third stage is defined as the critical mass loss in this study. The critical mass loss was concentrated between 7.5% and 8.5% of the fracture wires' mass loss. In addition, although 70-10-3 occurred brittle failure, its fracture type was the split type, no necking phenomenon, and its deformation was the

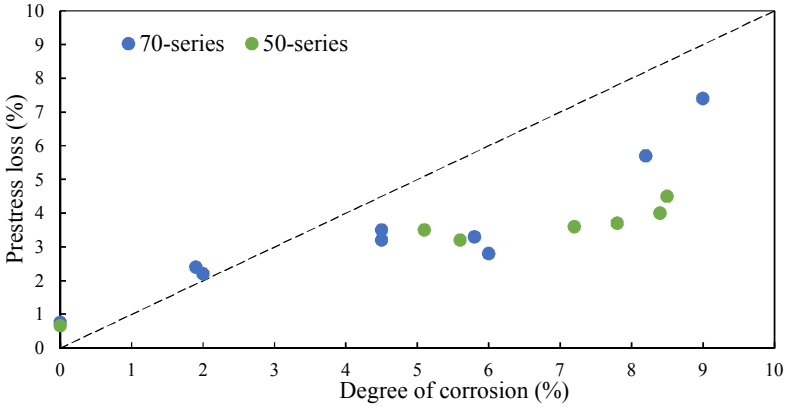


Fig. 11 Relationship between prestress loss and degree of corrosion.

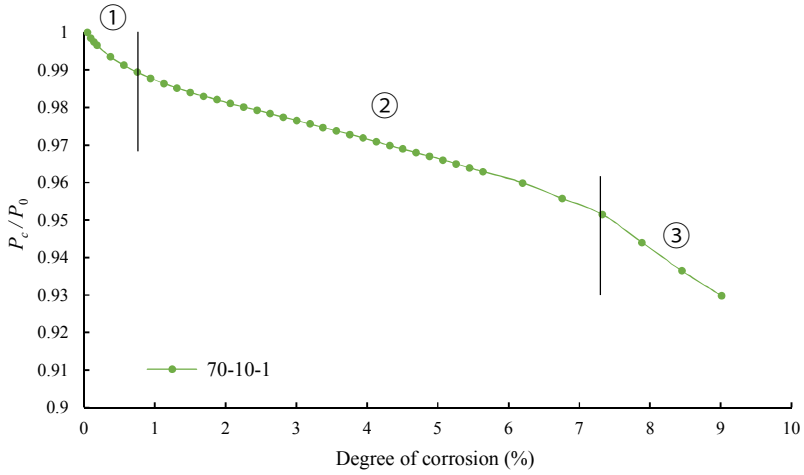


Fig. 12 Reduction process of prestressing force of corroded steel strand.

smallest. Thus, prestress loss of 70-10-3 seemed to be the least in the third stage.

3.7 A model for predicting prestressing force of corroded PC strands

The three stages of the prestress decline; the first stage mainly affects the prestress reduction factors are the relaxation performance of the strand as well as corrosion, while the relaxation performance of the strand is only related to time and has nothing to do with the degree of corrosion. In the third stage, the prestressing force is reduced due to a large amount of plastic deformation of the wire at the corrosion pit. The deformation depends on the different fracture modes of the strand, which occur randomly, so the prediction of the reduction of prestressing force becomes difficult. Therefore, this paper mainly studies the linear relationship between the second stage of prestressing force and the degree of corrosion. Separate interception of two prestress level specimens after 24 hours of corrosion time and the strand did not occur in the third stage of the test data are summarized in **Fig. 14**. According to the figure, the model of prestressing force and degree of corrosion relationship is assumed to be a liner equation. The test data for the 70-series and 50-series specimens were fitted and calculated.

$$P_c / P_2 = -0.42n + 1.008 \tag{4}$$

where P_c is the prestressing force of the steel strand after corrosion (kN); n is the degree of corrosion of the steel strand, and it is greater 2.0%; P_2 is the prestress load at 2% degree of corrosion (kN).

It can be seen from **Fig. 14** that the test data were used for verification and the proposed model had a good prediction accuracy, which can be employed to predict the prestress-degree of corrosion curve of corroded PC steel strands.

3.8 Nominal elastic modulus

Regarding how corrosion reduces the prestress of the strand, it is conjectured that corrosion leads to a reduction in the elastic modulus of the strand, which deforms and reduces its prestress. The modulus of elasticity of the test strand was calculated by the following equation.

$$E = \frac{\sigma}{\varepsilon} = \frac{F / A}{\Delta L / L_0} \tag{5}$$

where F is the prestressing force; A is an initial cross-sectional area that is not reduced due to corrosion; ΔL is the elongation; L_0 is the original length of specimens.

The following equation is the elastic calculation for-

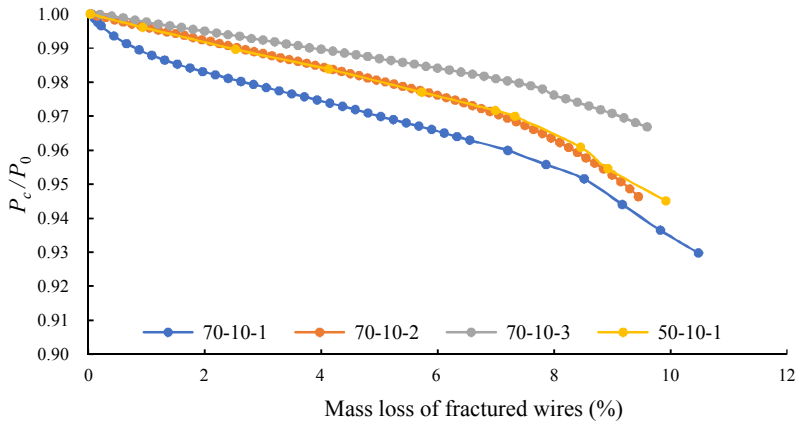


Fig. 13 Prestress ratio versus degree of corrosion obtained by Eq.(3) for corroded steel strands that fractured during the corrosion test.

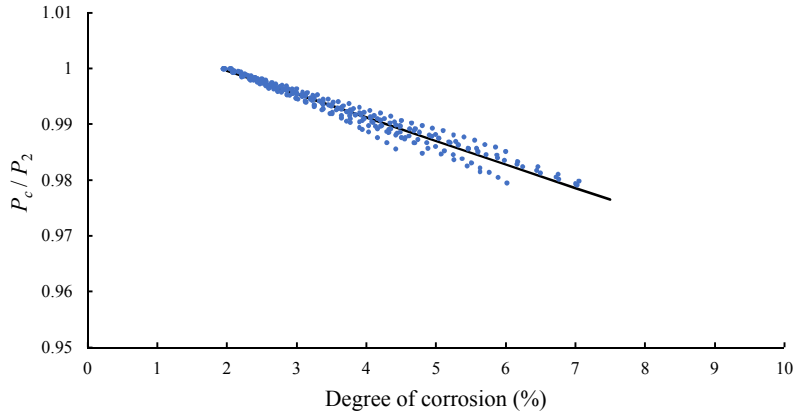


Fig. 14 Relationship between prestressing force and degree of corrosion.

mula, where K is the elasticity coefficient.

$$K = F / \Delta L \tag{6}$$

From Eqs. (5) and (6), the formula of the elasticity coefficient and elastic modulus of PC strand can be written as below.

$$K = E \cdot A / L_0 \tag{7}$$

Corrosion caused the cross-section loss and nominal elastic modulus declined. When the mass loss of steel strands is in the similar level, it can be assumed that average cross-sectional area loss is the same. According to Eq. (7), the lower elastic modules, the lower elasticity in this test, when the cross-sectional area of a PC strand is the same, and its initial length is constant. This decrease in the nominal elasticity of the PC strand leads to prestress loss. Thus, the prestressing force decreases continuously with the decrease of the nominal elastic modules of the PC strand.

The ratio of the elastic modulus after corrosion to the elastic modulus before corrosion of specimens with different degrees of corrosion is used to represent elastic properties. The mass loss was measured, and the ratio of elastic modulus was calculated when the corrosion test terminated. The influence of degree of corrosion on the elastic modulus is observed, as shown in **Fig. 15**. The results include the elastic modulus ratio of the uncorroded strand in this figure. The results show that there is a small decrease in the modulus of elasticity with the increasing degree of corrosion for both 70-series and 50-series, while that of 70-series decreased further at the degree of corrosion of around 8% or more.

4. Results and discussion in tensile loading tests

4.1 Failure mode

The tensile loading test was carried out on the nine steel strands that were not ruptured during the corrosion test. The fractography on the fracture surfaces of corroded steel wires with different degrees of corrosion was conducted after the tensile loading tests. The fracture sur-

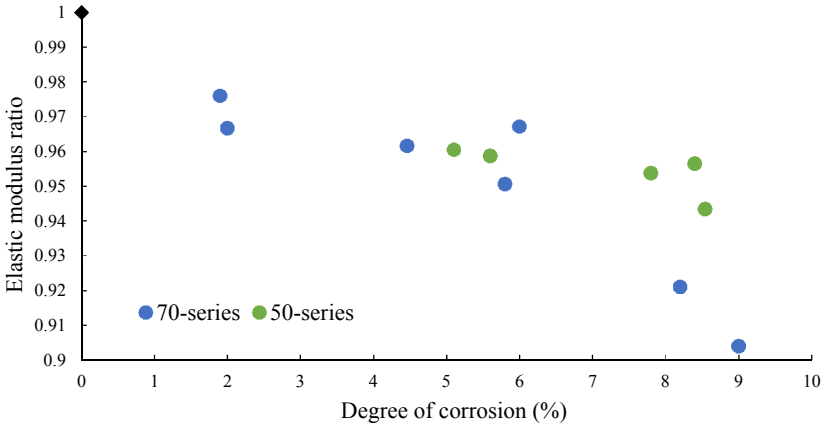
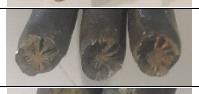
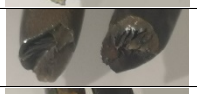
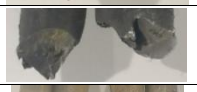
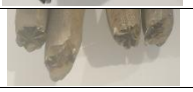


Fig. 15 Relationship between elastic modulus ratio and degree of corrosion.



Fig. 16 Fracture section of corroded steel wires after tensile loading test.

Table 6 Fracture condition of corroded steel wires after tensile loading test.

Specimen No-.	Fracture section	Fracture types	Necking degree	Mass loss of fractured wire (%)	Ultimate tensile capacity (kN)
70-2-1		Split-milling cutter type	Slight	2.7	187
70-2-2		Milling cutter type	Severe	3.7	223
70-5-1		Milling cutter type	Severe	6.2	215
70-5-2		Split-milling cutter type	Severe	5.0	223
70-5-3		Split-milling cutter type	Slight	5.3	208
50-5-1		Split type	None	5.9	188
50-5-2		Split type	None	6.2	202
50-5-3		Split-milling cutter type	Medium	7.5	204
50-10-2		Milling cutter type	Severe	8.8	197

faces are shown in **Fig. 16**. The fracture surface of uncorroded steel wire exhibits a necking phenomenon, which can be considered as a ductile fracture. After the corrosion test, the maximum tensile strength of the steel strand decreases, and also the failure mode changes from ductile failure to brittle failure. There is no obvious necking phenomenon at the fracture of steel strand. The results of the tensile test indicated that the corroded strands failed at the location with the minimum cross-sectional area. Thus, the degree of corrosion in the tensile test section is indicated by the mass loss of fractured wires, which is closer to the maximum cross-sectional area loss.

4.2 Ultimate tension capacity of corroded strand

The tensile test results are summarized, and the relationship between the ultimate tensile capacity and the degree of corrosion for the steel strand is shown in **Fig. 17**. Compared with the uncorroded steel strand (0%) of which the ultimate tensile capacity was 265 kN, the tensile capacity of the corroded steel strand was obviously decreased, but there was no obvious rule in the change of ultimate tensile properties with the increase of the mass loss of the fracture wires. The fracture section of specimens and ultimate load for each specimen are summarized in **Table 6**, in addition to the max mass loss as the degree of corrosion.

According to **Table 6**, the degree of corrosion of

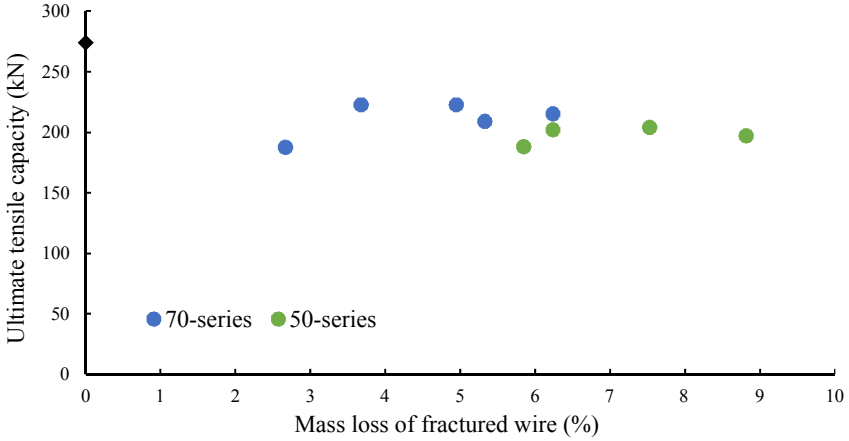


Fig. 17 Relationship between ultimate tensile capacity and mass loss of fractured wire.

70-2-1 was 2.67%, and the ultimate tensile capacity was only 187 kN; the degrees of corrosion of 70-5-1 and 50-5-2 are both 6.24%, but their ultimate tensile loads differ by 6.5%. Observing the fractures, it can be found that 70-2-1 and 50-5-2 are split type, which is a brittle fracture; 70-5-1 is a milling-cup cone type, which is a ductile fracture.

The ductile fracture originates from the plastic deformation that occurs first at the corrosion pitting. Subsequently, a more sufficient redistribution of stress and strain occurs in each section in which the corrosion pitting occurs in the wire. In contrast, brittle fracture originates from cracking caused by localized plastic deformation at the bottom of the corrosion pitting. And once cracked, rapid destabilization extends to full section fracture, namely, the initial fracture and limit fracture occur almost simultaneously. Therefore, the ultimate tensile strength of the wire with a split fracture is lower than other fracture types. When the degree of corrosion is the same, the ultimate tensile capacity of the strands with split fracture type brittle failure is lower.

Therefore, the fracture mode determines the ultimate tensile resistance of the steel strand. The different fracture modes of corroded steel wire in the strand depend on the fracture effect characteristics of the corrosion pitting, and the characteristics of fracture effect depend on the geometric characteristics of corrosion pitting. However, corrosion is random, and it is a probabilistic problem that corrosion pits lead to split fractures. Therefore, the relationship between degree of corrosion and ultimate tensile capacity was not obvious for this test.

5. Conclusions

The corrosion test and tensile test for fourteen 1×7 PC steel strands sustaining prestressing levels of 70% and 50% of tensile strength of PC strands were carried out to study the prestressing force and the residual properties of the corroded steel strand. The following conclusions were drawn:

1. The two series of prestress levels have a similar behavior of prestressing force reduction due to the corrosion. However, the prestress loss was slightly larger in 70-series than in 50-series at the corrosion level of around 8% or more.
2. The corrosion test with a sustained tensile force showed that the prestress deterioration process of corroded strand can be divided into three stages. In the first stage, the prestressing force decreased rapidly due to a relaxation of the steel strand. In the second stage, the prestressing force decreased linearly as increasing degree of corrosion. As for the third stage, with the increase in the degree of corrosion, the maximum cross-sectional area of the strand was severely reduced. In this stage, the tensile properties were reduced.
3. When the mass loss of the fracture wires does not exceed the critical mass loss, the prestressing force decreases linearly as the increase of mass loss of the steel strand. When the mass loss of the fracture wires exceeds the critical mass loss, the steel strand has a large plastic deformation at the corrosion pitting, and prestressing force drops rapidly. The critical mass loss was concentrated between 7.5% and 8.5% in the corrosion test.
4. Corrosion leads to a decrease in the ultimate tensile capacity of the strand and results in the failure mode transforming from plastic failure to brittle failure. The fracture was divided into milling cutter type, cup and cone type, and split type. The geometric characteristics of the corrosion pit determine the fracture mode of the wires and have an important effect on the ultimate tensile properties of corroded steel strands.

Acknowledgments

This research was partially supported from the Japan Society for the Promotion of Science (JSPS), Grant-in-Aid for Scientific Research (B), 19H02226 and Research Committee on Technological Development for Infrastructure.

References

Biondini, F. and Frangopol, D. M., (2018). "Life-cycle performance of civil structure and infrastructure systems: Survey." *Journal of Structural Engineering*, 144(1), 06017008.

Cederquist, S. C., (2000). "Motor speedway bridge collapse caused by corrosion." *Materials Performance*, 36(7), 18-19.

Darmawan, M. S. and Stewart, M. G., (2007). "Effect of pitting corrosion on capacity of prestressing wires." *Magazine of Concrete Research*, 59(2), 131-139.

Hong, S., Zheng, F., Shi, G., Li, J., Luo, X., Xing, F., Tang, L. and Dong, B., (2020). "Determination of impressed current efficiency during accelerated corrosion of reinforcement." *Cement and Concrete Composites*, 108, 103536.

Jeon, C., Lee, J., Lon, S. and Shim, C.-S., (2019). "Equivalent material model of corroded prestressing steel strand." *Journal of Materials Research and Technology*, 8(2), 2450-2460.

Kim, J. K., Kim, J. S., Kwon, S. H., (2014). "Mechanical properties of a new prestressing strand with ultimate strength of 2160 MPa." *KSCE Journal of Civil Engineering*, 18(2), 607-15.

Kitano, Y., Watanabe, H., Suzuki, S. and Tokumitsu, S., (2007). "Research on PC bridge remodeling technology, Part 1: Study on mechanical properties of corroded prestressed steel." *Journal of Prestressed Concrete, Japan*, 49(5), 52-56. (in Japanese)

Kondo, T., Yokoi, K., Kaita, T. and Hosoi, K., (2016). "Mechanical properties of cut artificially PC strands." In: *Proceedings of the 25th Symposium on the*

Development of Prestressed Concrete, Kokura, Fukuoka Prefecture, Japan 20-21 October 2016. Tokyo: Japan Prestressed Concrete Institute, 25, 263-268. (in Japanese)

Kuga, S., Tanaka, Y., Yamaguchi, T. and Shimomura, T., (2012). "Mechanical properties of corroded PC strands and residual strength of pretensioned PC beams." In: *Proceedings of the 21st Symposium on the Development of Prestressed Concrete*, Otsu, Shiga Prefecture, Japan 24-26 October 2012. Tokyo: Japan Prestressed Concrete Institute, 21, 211-216. (in Japanese)

Lee, J., Lee, Y. J. and Shim, C.-S., (2020). "Probabilistic prediction of mechanical characteristics of corroded strands." *Engineering Structures*, 203, 109882.

Proverbio, E. and Ricciardi, G., (2000). "Failure of a 40 years old post-tensioned bridge near seaside." In: *Proceedings of the of the European Corrosion Congress Eurocorr 2000*, London 10-14 September 2000. London: Institute of Materials.

Wang, L., Zhang, X., Zhang, J., Ma, Y., Xiang, Y. and Liu, Y., (2014). "Effect of insufficient grouting and strand corrosion on flexural behavior of PC beams." *Construction and Building Materials*, 53, 213-224.

Wang, L., Li, T., Dai, L., Chen, W. and Huang, K., (2020). "Corrosion morphology and mechanical behavior of corroded prestressing strands." *Journal of Advanced Concrete Technology*, 18(10), 545-557.

Wei, L., Dong. Z., Cui, H., Tang, W. and Feng. X., (2021). "An experimental study on the influence of applied voltage on current efficiency of rebars with a modified accelerated corrosion test." *Cement and Concrete Composites*, 122, 104210.

Zhang, X., Wang, L., Zhang, J. and Liu. Y., (2017a). "Corrosion-induced flexural behavior degradation of locally ungrouted post-tensioned concrete beams." *Construction and Building Materials*, 134, 7-17.

Zhang, X., Wang, L., Zhang, J. and Liu. Y., (2017b). "Flexural behavior of bonded post-tensioned concrete beams under strand corrosion." *Nuclear Engineering and Design*, 313, 414-424.